Frontiers in Bioscience Landmark

Front. Biosci. (Landmark Ed) **2025**; 30(3): 28062
https://doi.org/10.31083/FBL28062

Original Research

A Quality by Design (QbD) Project of Human Dermal Fibroblast and its Therapeutic Effects on Managing Degenerative Intervertebral Disc Fibrosis in Rabbit and Cynomolgus Monkey

Li Zhou[1,†], Hongsheng Li[2,3,†], Chen Chen[2,3,†], Hao Yang[1], Guicheng Zhang[1], Qin Zhang[1], Mengnan Wen[1], Lei Shi[2,3], Tong Xing[2,3], Ming Fan[1], An Qin[2,3,*], Jie Zhao[2,3,*], Shen'ao Zhou[1,*]

[1]FibroX Therapeutics (Shanghai) Inc., 201203 Shanghai, China
[2]Shanghai Key Laboratory of Orthopaedic Implants, Department of Orthopaedic Surgery, Shanghai Ninth People's Hospital, Shanghai Jiao Tong University School of Medicine, 200011 Shanghai, China
[3]Shanghai Jiao Tong University School of Medicine, 200025 Shanghai, China
*Correspondence: dr_qinan@163.com (An Qin); profzhaojie@126.com (Jie Zhao); shenao.zhou@celliver.com (Shen'ao Zhou)
[†]These authors contributed equally.
Academic Editor: Amancio Carnero Moya
Submitted: 8 November 2024 Revised: 22 December 2024 Accepted: 25 December 2024 Published: 12 March 2025

Abstract

Background: Low back pain (LBP) is the leading cause of disability among the elderly, placing significant social and economic burdens on societies globally. A common cause of chronic LBP is lumbar disc degeneration. Previously, we reported that autologous or allogenic fibroblast injections could treat intervertebral disc degeneration (IVDD) in preclinical studies by maintaining disc height and stability through fibrosis. However, the pathway to successful drug development remains unclear. **Methods**: To develop a novel human allogenic fibroblast injection, we launched a quality-by-design (QbD) project focusing on human dermal fibroblasts (HDFs). **Results**: We developed a tissue separation process, HDF culture process, and HDF cryopreservation process. The tissue disinfection method used 5% povidone-iodine solution and 75% alcohol for 3–5 min each; the tissue digestion conditions used neutral protease AF followed by overnight soaking plus collagenase NB6 digestion for 2–3 h; the non-animal component medium contained high glucose dulbecco's modified eagle medium (DMEM) + 7.5% human platelet lysate (hPL); A cell density of 14,000–18,000 cells/cm^2 was used; the cell cryopreservation solution contained 75% CS10 + 10% human serum albumin (HSA) + 15% saline (NaCl). Finally, we explored its therapeutic effects by treating IVDD in rabbits. **Conclusions**: The model of lumbar disc degeneration in rabbits was induced by acupuncture, and HDF was injected into the intervertebral disc. The therapeutic effect of HDF was observed by imaging and histopathology at 1, 3, and 6 months after administration. HDF treatment significantly improved the water content of degenerative intervertebral discs and maintained the height and stability of intervertebral discs. Signal pathway analysis in cynomolgus monkeys suggested that the primary mechanism involves promoting disc fibrosis. Therefore, this study demonstrated the feasibility and cost-effectiveness of manufacturing FibroCell^{TM}, a foreskin-derived human dermal fibroblast injection. FibroCell^{TM} shows promise as a cell-based therapy for IVDD treatment.

Keywords: lumbar/intervertebral disc (IVD); human dermal fibroblasts (HDFs); intervertebral disc degeneration (IVDD); low lack pain; cell therapy

1. Introduction

Low back pain (LBP) is a significant cause of disability in the elderly and places substantial social and economic burdens on societies globally [1,2]. One of the most common diagnoses associated with LBP is lumbar/intervertebral disc degeneration (IVDD), which leads to lumbar instability and height loss. These changes can result in symptomatic nerve compression, intervertebral foramen stenosis, adjacent segment degeneration, and instability-induced LBP [3–5].

Intervertebral disc degeneration is a progressive, cell-mediated process involving molecular, structural, and biomechanical changes. It begins in the nucleus pulposus (NP), where a reduction in proteoglycan content and a decrease in the proteoglycan-to-collagen ratio cause a loss of hydrostatic properties. This leads to structural wear and compromised biomechanical functions [6]. Current IVDD treatments, such as surgical interventions, aim to reduce symptoms and minimize lumbar disability [7]. Percutaneous endoscopic lumbar discectomy (PELD) is commonly used to relieve nerve root compression. Surgical interventions typically focus on maintaining intervertebral space stability and relieving severe neurological symptoms, often involving discectomy and interbody fusion. However, nucleus pulposus removal may risk a recurrence of disc herniation and late-stage intervertebral space height loss, causing spinal instability. Moreover, intervertebral disc fusion sacrifices lumbar spine mobility and accelerates adjacent intervertebral disc degeneration by shifting biomechanical

Copyright: © 2025 The Author(s). Published by IMR Press.
This is an open access article under the CC BY 4.0 license.

Publisher's Note: IMR Press stays neutral with regard to jurisdictional claims in published maps and institutional affiliations.

functions [8]. Therefore, there is an urgent need for more targeted and less invasive regenerative strategies, such as minimally invasive NP or AF treatments.

Given the limitations of current IVDD treatments, disc regeneration methods have gained increasing research attention [8,9]. Cell-based therapies, including allogeneic and autologous approaches, are attractive due to their ability to target multiple IVDD pathways. These cells can produce essential extracellular matrix (ECM) components, such as aggrecan, type I and II collagen, and fibronectin, which maintain disc stability [10]. Among various human cell types, fibroblasts are the most common structural support cells in the body to treat IVDD [11–15]. They can integrate into discs, accelerating fibrosis and maintaining disc height. Additionally, fibroblasts secrete growth factors like transforming growth factor-β (TGF-β) and fibroblast growth factor (FGF), which stimulate tissue-specific cell proliferation and enhance natural repair processes [16,17]. Several independent studies have demonstrated fibroblasts' potential in treating IVDD and reducing inflammation in rabbit and monkey models, generating significant clinical interest [18,19].

Our previous study has shown that autologous and allogenic fibroblast injection may serve as a potential treatment approach. Fibroblasts enhance the natural fibrosis process during acute and subacute stages of stress-induced IVDD [20]. Compared with the IVDD group, the fibroblast-treated group exhibited effective disc height maintenance, reduced endplate degeneration, and improved nuclear magnetic resonance signals and overall histological structure in rats, rabbits, and monkeys [21]. Long-term imaging data, including X-ray, computed tomography (CT), and magnetic resonance imaging (MRI), indicated that fibroblast injection significantly reduced osteophyte generation after one year. Fibrotic discs maintain the intervertebral space's stability, biological activity, and mechanical properties, thus presenting a new direction for treating lumbar degenerative diseases originating from the intervertebral space.

Developing a first-in-class human allogenic fibroblast injection must comply with pharmaceutical manufacturing standards and regulatory oversight. Quality by design (QbD) is a strategic method used across various industries, including pharmaceuticals, to produce high-quality products consistently. It integrates quality considerations throughout the entire product lifecycle, from initial concept to final production. In this study, we applied QbD to human dermal fibroblasts derived from teenager foreskin tissue. We produced a fibroblast cell injection and investigated its pharmacodynamic effects on treating IVDD in rabbits. The data from process development and quality-control studies provide a strong foundation for future clinical trials. Further analysis of signal pathways in intervertebral discs of cynomolgus monkeys suggested that the primary mechanism involves enhancing fibrotic pathways, thereby managing disc fibrosis. From an industry and clinical perspective, this work demonstrated the practicality and cost-effectiveness of a foreskin-derived human dermal fibroblast injection (FibroCell^{TM}) as a promising cell-based therapy for IVDD treatment.

2. Methods

2.1 Part I: Process Development

2.1.1 Isolation of Human Dermal Fibroblasts (HDFs)

The study design and volunteer recruitment were approved by the Ethics Committee of the Shanghai Ninth People's Hospital, Shanghai Jiao Tong University School of Medicine (approval number: SH9H-2021-T94-2 and SH9H-2023-T186-3). All experiments adhered to relevant guidelines and regulations.

Foreskin samples from individuals under 18 years old were obtained from circumcisions performed at Shanghai Ninth People's Hospital, Shanghai Jiao Tong University School of Medicine. The collected tissues were weighed, cleaned, and disinfected by soaking in 5% povidone-iodine solution (Shanghai Xiao Fang Pharmaceutical Co., Ltd., Shanghai, China) and 75% ethanol solution (China National Medicines Corporation Ltd., Beijing, China), each for 3–5 min. After disinfection, tissues were washed with PBS a minimum of three times. The tissues were then evenly distributed and transferred into either 2 mg/mL Dispase II (Roche, Basel, Switzerland) or 2 DMC U/mL Neutral protease AF (Nordmark, Uetersen, Germany) and left to stand at 4 °C for 10–20 hours. Following this, the dermal tissue was separated from the whole skin layer, cut into ~1 mm^3 pieces, and immersed in different collagenases. The collagenases used were 2 mg/mL type XI collagenase (Sigma, St. Louis, MO, USA), 2 mg/mL type I collagenase (absin, Shanghai, China), or 0.1 PZ U/mL NB6 collagenase (Nordmark, Uetersen, Germany). The tissues were then digested in a 37 °C incubator (ESCO, Singapore) for 2–3 h with oscillation using a cell culture shaker (DLAB, Beijing, China). After digestion, the optimal digestion conditions were determined based on the number of viable cells. Alternatively, the defined process procedures allowed the whole foreskin tissue to be directly cut and digested in the desired collagenase, omitting the epidermis removal process. All primary cells were validated for their identity by surface marker analysis using flow cytometry and tested negative for mycoplasma.

2.1.2 Screening of Animal-Component-Free (ACF) Culture Medium or FBS Substitute

Conventionally, fibroblasts are cultured in high-glucose dulbecco's modified eagle medium (DMEM, Thermo Fisher Scientific, Waltham, MA, USA) supplemented with Fetal Bovine Serum (FBS) [22]. We screened commercial FBS substitutes compatible with fibroblast culture to find a suitable animal-component-free (ACF) culture medium. The candidates were: human platelet

lysate (hPL, Sexton, Indianapolis, IN, USA), Ultroser G Serum Substitute (Sartorius, Göttingen, Germany), Xerum-Free XF212 (amsbio, Oxfordshire, UK), KnockOut SR XenoFree (Thermo Fisher Scientific, Waltham, MA, USA), KBM Fibro Assist (KOHJIN BIO, Tokyo, Japan), and Fibroblast Medium-animal component free (FM-acf, ScienCell, San Diego, CA, USA). The number of harvested cells and culture time were recorded.

2.1.3 Optimization of Cultural Media

Seven basal media were tested, including DMEM, RPMI-1640, DMEM/F-12, MEM, McCoy's 5A, Human Fibroblast Expansion Basal Medium (all from Thermo Fisher Scientific, Waltham, MA, USA), and Fibroblast Growth Basal Medium (Lonza, Basel, Switzerland). Different concentrations of FBS substitute (3%, 5%, 7.5%, and 10% hPL) were also tested. The culture time and harvested cell number were recorded for each combination.

2.1.4 Optimization of Cell Seeding Density

Three fibroblast seeding densities were tested: 14,000 cells/cm^2, 18,000 cells/cm^2, and 22,000 cells/cm^2. The culture duration and harvested cell number were recorded for each density.

2.1.5 Optimization of the Cell Cryopreservation Solution

To optimize cell recovery and viability, we tested five cell cryopreservation formulas: CS-10 (Biolife Solutions, Bothell, WA, USA), 75% CS-10 + 10% HSA (CSL, Melbourne, Australia) + 15% NaCl (Cisen Pharmaceutical Co., Ltd., Jining, China), 90% CS-10 + 10% HSA, 1% TG-40 + 10% HSA + 10% DMSO + 79% NaCl, and 1% TG-40 (Sichuan Kelun Pharmaceutical Co., Ltd., Chengdu, China) + 40% hPL+10% DMSO + 49% NaCl (v/v). Cells were cooled according to a program and stored in a –80 °C refrigerator (Thermo Fisher Scientific, Waltham, MA, USA). Cell viability and the number of viable cells were assessed post-thawing after 7, 14, 30, 60, and 90 days of storage.

2.1.6 Procedure Robustness and Process Repeatability Research

Process parameters for the separation, culture, and cryopreservation of human dermal fibroblasts (HDFs) derived from foreskins were confirmed, and a production roadmap was developed. Eight batches of HDFs from eight different donors were produced on a small scale using these processes. HDFs were isolated from foreskin tissue using two methods: five tissues (donors 1, 2, 4, 7, 8) were digested with neutral protease AF overnight before the dermis was isolated and digested with collagenase, while three tissues (donors 3, 5, 6) were directly digested with collagenase. All primary cells were cultured to passage 8 (P8) for clinical use, and a secondary cell bank was established during this process. The cell seeding numbers, harvested cell counts, and culture durations per passage were recorded to assess HDF proliferation ability and demonstrate production process robustness.

2.1.7 Mathematical Statistics

Cell expansion fold, population doubling level (PDL), and doubling time (DT) were calculated to analyze cell proliferation under different conditions. PDL values were positively correlated to the proliferation ability, while DT values were inversely correlated. The cell expansion fold was determined by dividing the harvested cell number by the seeding cell number. The total cell number was calculated by multiplying the initial cell amount by the cell expansion fold per generation.

PDL and DT were calculated using the following formulas (where N_0 is the seeding cell number, N_1 is the harvested cell number, and T is the incubation time).

PDL = $log10(N_1/N_0) * log2(10)$

DT = $log10(2)/log10(N_1/N_0) * T$

2.2 Part II Preclinical Study

2.2.1 Animals Welfare

The HDFs used in animal experiments were sourced from one of the aforementioned small-scale productions. The animal experiments were approved by the Animal Committee (approval number JGLL-20220601 for rabbits and IACUC-2024-538 for cynomolgus monkeys). During the experiments, Cynomolgus monkeys were anesthetized with an intramuscular injection of 0.05 mg/kg atropine sulfate (0.5 mg/mL, Minsheng Pharmaceutical Co., Ltd, Hangzhou, China) and 0.3 mL/kg Zoletil 50 (250 mg/mL, Virbac, Carros, France), and were euthanized by bloodletting following anesthesia. New Zealand rabbits were anesthetized with an intramuscular injection of 0.3 mL/kg Zoletil 50 (250 mg/mL) and euthanized by bloodletting following anesthesia. All experiments adhered to relevant guidelines and regulations.

2.2.2 Pharmacodynamic Study on Rabbit Model

Sixteen male New Zealand rabbits, aged 6 months with a mean weight of 2.5 $\pm$ 0.5 kg, were obtained from Jiagan Biotechnology Corporation (Shanghai, China). The rabbits' back and abdomen hair were removed, and they were placed in the right lateral position. The abdominal skin and muscles were incised to expose the intervertebral discs. The animals were then assigned to sham and experimental groups. For the sham group, intervertebral disc L2/3 was used. For the experimental groups, discs L3/4, L4/5, and L5/6 were employed. The intervertebral disc degeneration was induced using a 20-gauge needle via negative pressure puncture. The needle was inserted to a depth of 4 mm and withdrawn after one rotation. Following this procedure, disc L4/5 was injected with 20 µL of solvent. Disc L3/4 and L5/6 were injected with HDFs at concentrations of 5 $\times$ 10^5 cells/20 µL and 2 $\times$ 10^6 cells/20 µL in the first 8 animals, disc L3/4 and L5/6 were injected with HDFs at

concentrations of 2×10^6 cells/20 μL and 5×10^5 cells/20 μL in last 8 animals, respectively. Post-operation, the skin incisions were sutured and disinfected. Due to the death of an animal during surgery, only 15 animals were involved in the subsequent tests.

2.2.3 Magnetic Resonance Imaging (MRI) and Computed Tomography (CT) Analysis

All animals underwent MRI and CT scans at 1, 3, and 6 months post-treatment. 15 animals involved in MRI and CT detection at 1, 3 months, as 3 animals were sacrificed for histological detection at 3 months only 12 animals were involved in MRI and CT detection at 6 months. MRI was performed using a UMR580 (UNITED IMAGING, Shanghai, China) with the following parameters: repetition time (TR) of 1800 ms, echo time (TE) of 98 ms, slice thickness 1.1 mm, slice interval 0.22 mm, field of view (FOV) 160 mm × 65 mm, and voxel size 0.25 mm × 0.25 mm × 1.1 mm. CT scans were conducted using a UCT528 (UNITED IMAGING, Shanghai, China) with a spatial resolution of 1.0 mm, voltage of 120 kV, and electrical current of 200 mA. The disc height index (DHI) indicates the intervertebral disc height, calculated as the disc height measurements multiplied by 2 and divided by the average height of the two adjacent vertebral bodies. The gray value, representing the intervertebral disc's water content, was derived from the MRI index and measured using Analyze 14.0 software (AnalyzeDirect, Overland Park, KS, USA). All images were measured by three independent observers unaware of the sample, and the average of their assessments was recorded.

2.2.4 Histopathologic Analyses

At three months post-treatment, three rabbits were randomly selected and euthanized. Their lumbar intervertebral disc specimens were fixed in formaldehyde (Servicebio, Wuhan, China), embedded in paraffin, and serially sectioned. The tissues were dewaxed, rehydrated, and stained with Safranin O-Fast Green (SOFG, Servicebio, Wuhan, China) and Hematoxylin and Eosin (H&E, Servicebio, Wuhan, China) staining. An Olympus microscope (Olympus, Tokyo, Japan) captured these images. Three independent observers, blinded to the group details, calculated the height of the intervertebral discs in each group.

2.2.5 Safety Research on Cynomolgus Monkey Model

Four cynomolgus monkeys (two males and two females, aged 4.1–6.3 years) were sourced from Guoke Saifu Hebei Pharmaceutical Technology Co., Ltd. The safety evaluation of HDF injection was conducted at this institution. Monkeys were randomly assigned to low-dose (3×10^6 cells/IVD) and high-dose (1.2×10^7 cells/IVD) groups. A 22G puncture needle (ESSICA, Taizhou, China) was used to percutaneously insert into the nucleus pulposus of the L5/6 intervertebral disc of each monkey. After removing the needle core, a micro-syringe was connected to inject 0.1 mL of HDF. Post-injection, animals were continuously observed for four weeks, with the day of administration designated as Day 1 (D1). Daily observations of the general state of all surviving animals were conducted, with detailed clinical observations occurring weekly. Body weight, food intake, and body temperature (rectal temperature) were measured weekly. ECG measurements were taken 3 h post-administration and at the end of the observation period. Cytokine levels were measured at 4 h, 24 h, and D29 post-administration. At the end of the observation period (D29), hematology, blood biochemistry, CRP, blood coagulation, and urine tests were performed. Animals were then euthanized for gross anatomical observation and pathological examination. Additionally, the nucleus pulposus (NP) and annulus fibrosus (AF) of the injected and non-injected IVD of two animals were collected for bulk RNA-seq to study the effect of HDF injection on IVD tissue cells. Primer sequences and supplementary methods are shown in the **Supplementary Materials**.

2.2.6 Statistical Analysis

The number of biological replicates and technical repeats in each experimental group is indicated in figure legends. The experimental design incorporated user blinding when possible. Compiled data are expressed as mean ± standard deviation (SD). For comparison between two groups, a two-tailed unpaired Student's *t*-test was used when variances were similar (tested with F-test), whereas a two-tailed unpaired Student's *t*-test with Welch's correction was used when variances were different; for multiple comparisons, a one-way ANOVA test was used, followed by Dunnett's post-test when comparing each group to the control group, or followed by Tukey's post-test when comparing all pairs of groups. Statistical analyses were performed using GraphPad Prism (V8.0, Boston, MA, USA) software. $ns > 0.05$; $*p < 0.05$; $**p < 0.01$; $***p < 0.005$; $****p < 0.0001$.

3. Results

3.1 The Isolation Process and Culture Medium Selection of Human Dermal Fibroblast

The "Guidelines for Pharmaceutical Research and Evaluation of Human Stem Cell Products" clearly states that animal-derived materials should be avoided in the production of cell therapy products. Instead, animal-component-free materials with defined components should be used where possible. To align with these guidelines, various combinations of digestive enzymes and animal-free media were employed to develop a method for isolating and culturing human dermal fibroblasts. Donor foreskin dermal tissues weighing around 1–2 g were divided into four parts for testing different enzyme combinations. After digesting tissues from three donors using neutral protease AF and NB6 collagenase, approximately 2.0×10^6 cells were harvested. Furthermore, these enzymes, being commercial

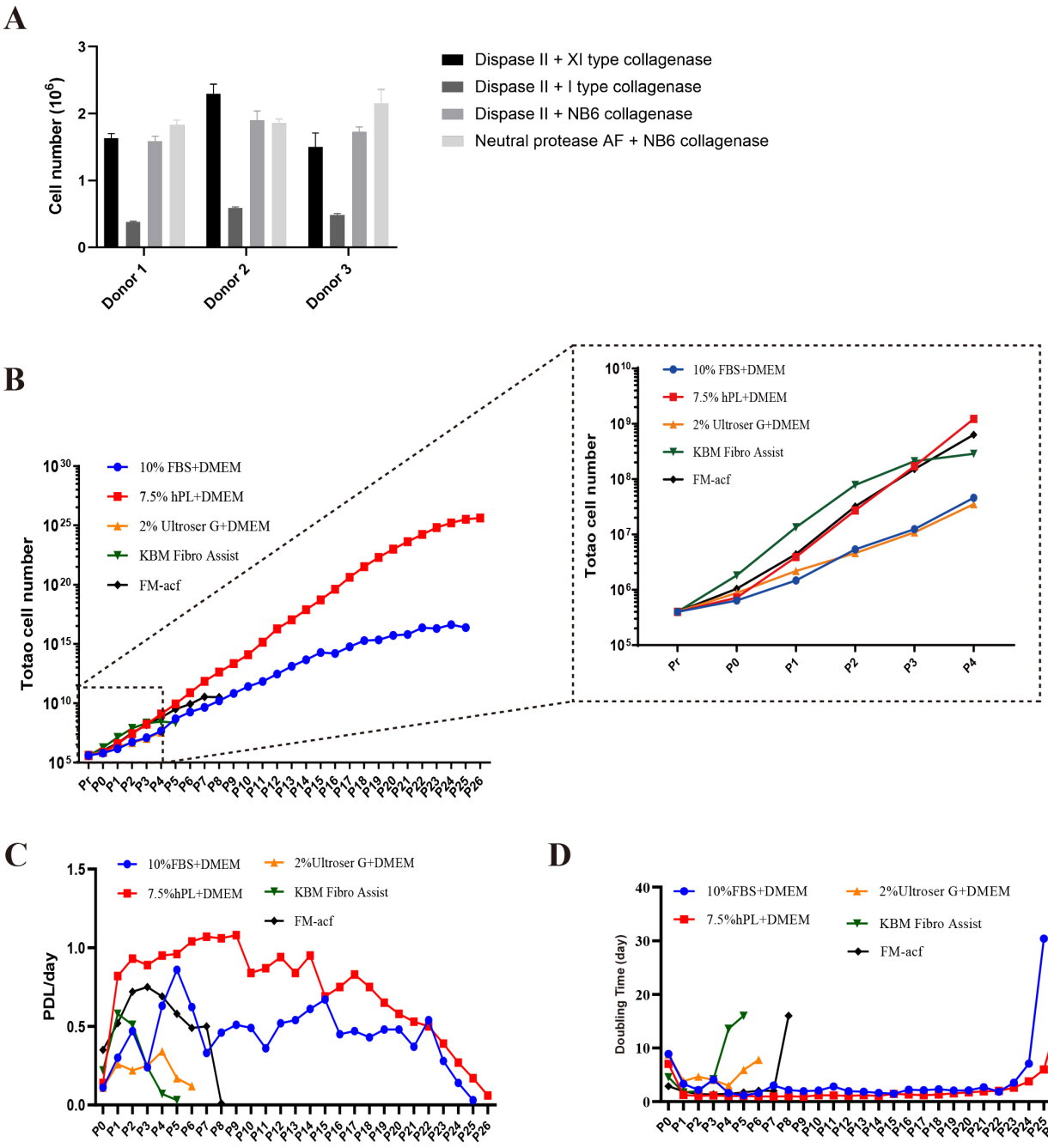

Fig. 1. The isolation process and culture medium selection of human dermal fibroblast. (A) The number of human dermal fibroblasts (HDFs) obtained from three donors using four digestive enzyme combinations for isolation. (B) Total HDF counts grown with five types of media over 26 passages (left) and enlarged pictures of cells from the first four generations (right). (C) Population doubling level per day (population doubling level (PDL)/day) of HDFs cultured in five media types over 26 passages. (D) Doubling time of HDFs grown in five media types over 26 passages.

GMP-grade, proved to be the most suitable combination for isolating fibroblasts from children's foreskin for future manufacturing processes (Fig. 1A).

Next, four serum substitutes and two commercial ACF culture media were evaluated to identify the optimal non-animal component culture medium for HDF. Isolated HDFs were seeded at equal densities into T25 culture flasks. Cells cultured in XerumFree XF212 and KnockOut SR XenoFree media failed to adhere and proliferate. After four passages, HDFs in 2% Ultroser G + DMEM, KBM Fibro Assist, and FM-acf also ceased proliferating (Fig. 1B, right, zoom-in picture). In contrast, 10% FBS + DMEM and 7.5% hPL + DMEM supported HDF growth for over 25 passages (Fig. 1B). Notably, 7.5% hPL + DMEM emerged as the op-

timal culture medium. In this medium, the total cell number (Fig. 1B), population-doubling level (PDL)/day (Fig. 1C), and doubling time (Fig. 1D) were significantly higher or faster than in other media. Moreover, HDFs could be cultivated in DMEM + 7.5% hPL for at least 25 passages (Figs. 1C,D).

The data above indicates that the combination of neutral protease AF and NB6 collagenase is optimal for isolating HDF from human foreskin, while DMEM + 7.5% hPL promotes the fastest cell expansion.

3.2 Optimization of Cultural Media and Cell Preservation Solution

Considering commercial cost and compliance, further tests were conducted to optimize the basal culture medium and the concentration of the FBS substitute. hPL was deemed the best alternative to FBS. Thus, seven types of basal media were tested with 7.5% hPL: DMEM, RPMI-1640, DMEM/F-12 (DF-12), MEM, McCoy's 5A, Human Fibroblast Expansion Basal Medium (Gibco basal), and Fibroblast Growth Basal Medium (Lonza basal).

Primary HDFs were divided into seven groups and seeded in T25 culture flasks with equal cell numbers. After five passages, HDFs grown in DMEM showed the fastest expansion, with a total cell number of approximately 8 $\times$ 10^9 (Fig. 2A), the highest PDL/day (Fig. 2B), and the shortest doubling time (Fig. 2C). These results suggest that DMEM is the most suitable basal medium for culturing HDFs.

Additionally, a gradient of hPL concentrations (from 3.0% to 10%) was tested to determine the optimal concentration. Compared with other concentrations, HDF grown in DMEM + 10% hPL and DMEM + 7.5% hPL showed faster PDL/day (Fig. 2D) and shorter doubling times (Fig. 2E), with higher total cell numbers at passage 5 (Fig. 2F). Regarding commercial cost and compliance, DMEM + 7.5% hPL is the most suitable medium for clinical HDFs.

Accordingly, the cell density of HDFs was adjusted, as their growth relies on autocrine cytokines. Both low and high seeding densities can negatively impact large-scale production. Cells were seeded at different densities (from 14,000/cm^2 to 22,000 cm^2) per passage, and their PDL/day, total cell number, and doubling time were calculated. Fig. 2G–I shows that the optimal seeding density for HDF culture and large-scale production is between 14,000 cells/cm^2 and 18,000 cells/cm^2, within which HDFs exhibit the highest proliferation rate.

The formulation of the cryopreservation solution impacts cells' post-thaw viability and recovery rate. Several formulations were tested, including CS-10 alone, 75% CS-10 + 10% HSA + 15% NaCl, 90% CS-10 + 10% HSA, 1% TG-40 + 10% HSA + 10% DMSO + 79% NaCl, and 1% TG-40 + 40% hPL + 10% DMSO + 49% NaCl (v/v). HDFs were cryopreserved at an equal cell density and stored at –80 °C for 7, 14, 30, 60, and 90 days. After thawing in a 37 °C water bath, the formulation of 75% CS-10 + 10% HSA + 15% NaCl demonstrated the best cell viability and viable cell number (Fig. 2J,K).

These data confirm that the most suitable culture medium for HDFs is DMEM basal medium supplemented with 7.5% hPL, with an optimal seeding density of 14,000 cells/$cm^2$to 18,000 cells/cm^2. Furthermore, the formulation of 75% CS-10 + 10% HSA + 15% NaCl is the most effective for HDF cryopreservation, yielding better cell viability and viable cell numbers.

3.3 The Robustness of Production Engineering

We conducted eight batches of HDFs and cultured them to the P8 generation on a small scale. During this process, we established the main cell bank (MCB) and working cell bank (WCB). We recorded the number of harvested cells, seeding cells, and culture days to determine the cells' proliferation ability. Our results indicated no significant differences in the growth curves of the eight batches, including total cell number, population doubling level (PDL), and doubling time. This consistency proved the stability of the HDF separation, culture, and cryopreservation processes (Fig. 3A–C). Additionally, we examined the impact of epidermis separation on the yield of primary fibroblasts and their proliferation abilities. Tissues from donors 1, 2, 4, 7, and 8 were digested with neutral protease overnight, followed by dermis isolation and collagenase digestion. Meanwhile, tissues from donors 3, 5, and 6 were directly digested with collagenase to isolate HDFs. The summarized data in Fig. 3D,E demonstrated that epidermis separation did not affect HDF proliferation ability (doubling time) or cell morphology. Blue lines represent cells derived from foreskins with separated epidermis, while red lines indicate those without separation.

3.4 Gene Expression and Protein Secretion Level of HDF

After establishing the complete production method for isolating and preserving HDFs, we isolated and cultured HDFs from eight donors. To compare HDFs with the human foreskin fibroblast cell line HFF-1, we selected several key gene markers. α-*SMA* an identical marker for fibroblasts [23], facilitates tissue repair and biomechanical remodeling [12]. *VIMENTIN*, *DESMIN*, *FIBRONECTIN*, *COL3A1*, and *COL1A1* are extracellular matrix (ECM) components that stabilize IVDD [24]. Additionally, we detected other fibroblast markers such as *CD26*, *THY-1* (*CD90*), *FAP*, and Fibroblast Specific Protein-1 (*FSP-1*) [25] using qRT-PCR. HDFs from 8 eight donors were continuously passaged eight times. At the end of the eighth passage, we collected the cultured media and performed ELISA assays to test the secretion of TGF-β1 and COL1A1.

All tested genes, including α-*SMA*, *TGF-β1*, *VIMENTIN*, *THY-1*, *FSP-1*, *FIBRONECTIN*, *COL3A1*, *DESMIN*, *DDR2*, *FAP*, *COL1A1*, and *CD26* were ex-

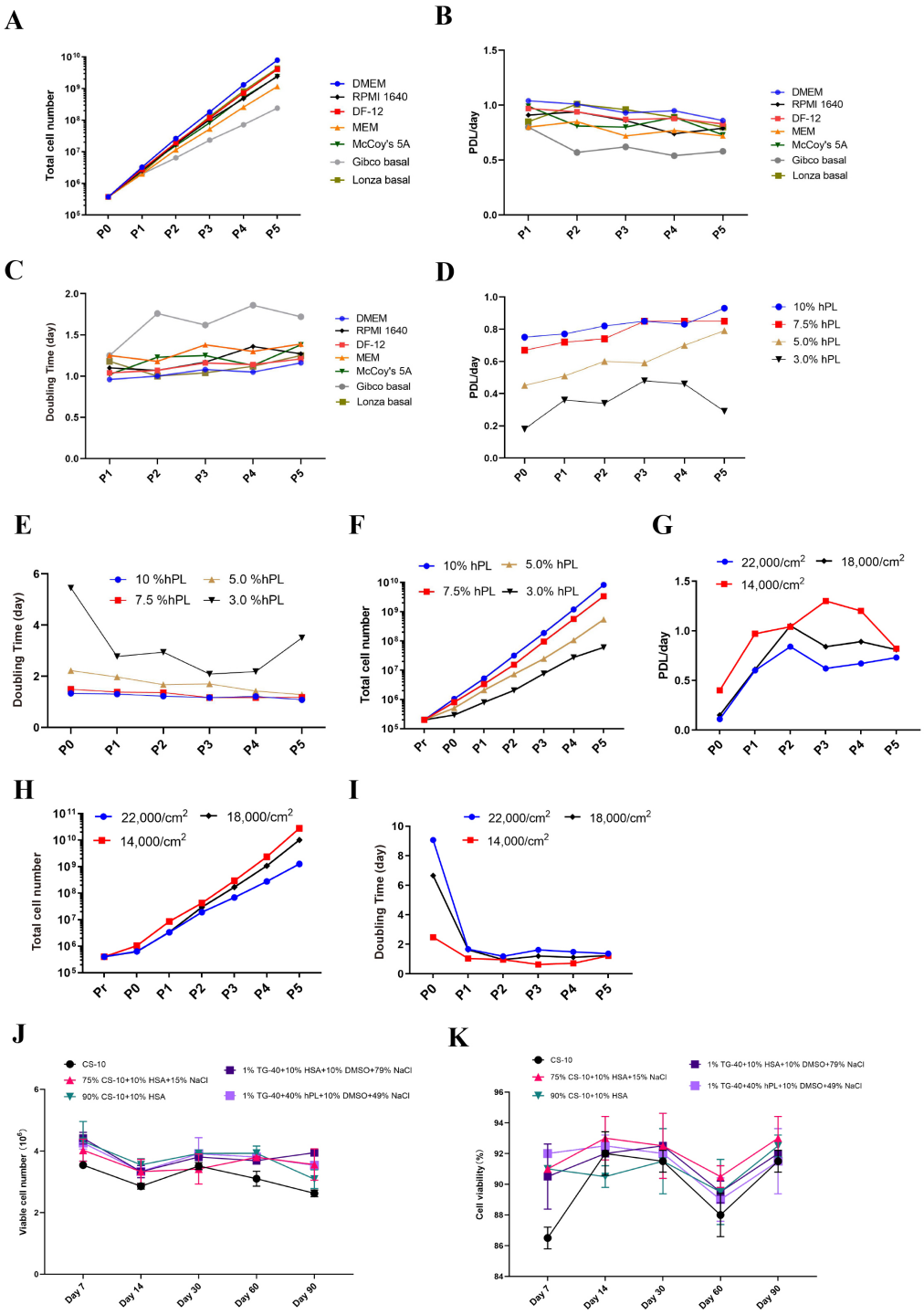

Fig. 2. Optimization of cultural media and cell preservation solution. (A) Total cell count of HDFs cultured in combination with seven basal media and human platelet lysate (hPL) for five passages. (B) PDL/day of HDF grown with a combination of seven basic media and hPL for 5 passages. (C) Doubling time of HDFs grown in combinations of seven basal media and hPL for five passages. (D) PDL/day of HDFs cultured with 3%, 5%, 7.5%, or 10% hPL for five passages. (E) Doubling time of HDFs cultured with 3%, 5%, 7.5%, or 10% hPL for five passages. (F) Total cell count of HDFs cultured with 3%, 5%, 7.5%, or 10% hPL for five passages. (G) PDL/day of HDFs cultured at three different seeding densities for five passages. (H) Total cell count of HDFs cultured at three different seeding densities for five passages. (I) Doubling time of HDFs cultured at three different seeding densities for five passages. (J) Number of viable HDFs recovered after cryopreservation with five different solutions at Days 7, 14, 30, 60, and 90. (K) Viability of HDFs recovered after cryopreservation with five different solutions at Days 7, 14, 30, 60, and 90.

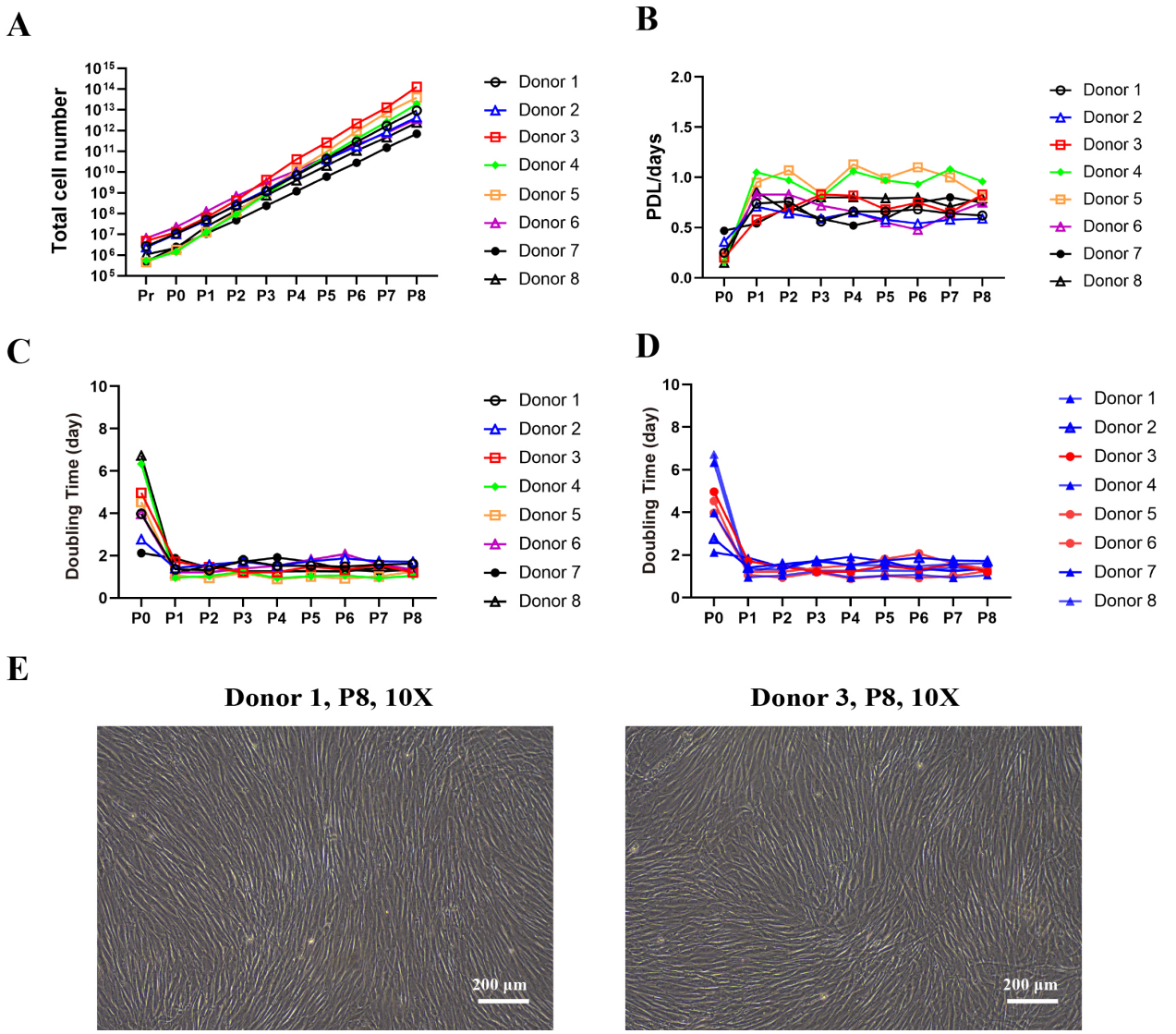

Fig. 3. The robustness of production engineering. (A) Total cell number of human dermal fibroblasts (HDFs) isolated from eight donors and cultured over eight passages. (B) PDL/day of HDFs isolated from eight donors and cultured over eight passages. (C) Doubling time of HDFs isolated from eight donors and cultured over eight passages. (D) Doubling time of HDFs isolated from eight donors and cultured over eight passages. Blue lines represent cells derived from foreskins where the epidermis was removed, while red lines represent cells where the epidermis was intact. (E) Morphology of HDFs isolated from donors 1 and 3 at P8. Scale bars, 200 μm.

pressed in HDFs at approximately the same level as in the control cell line HFF-1 [26]. Some donors (e.g., donor 1 and donor 2) even showed higher expression levels than HFF-1 (Fig. 4A). ELISA tests also revealed similar secretion levels of COL1A1 and TGF-β1 in HDFs from eight donors (Fig. 4B). This indicates that our isolation and culturing methods for HDFs maintain the gene expression and protein secretion patterns *in vitro*. Furthermore, the separation of the epidermis did not affect the gene expression and protein secretion of HDFs.

3.5 Characteristics and Identification of HDFs

Flow cytometry (FCM) analysis was conducted to examine the surface and intracellular markers of HDF. The markers Vimentin, Fibronectin, FSP-1, α-SMA, Desmin, CD105, CD73, and CD90 were all positively expressed (>90%) in HDF (Fig. 5A and and Table 1). Conversely, the negative markers CD45, CD31, CD11b, and HLA-DR/DQ/DP were not expressed in any of the eight donors (Fig. 5B and and Table 1). These results suggest that the HDF cultured using our methods have high purity and low immunogenicity. Additionally, the separation of the epidermis did not affect HDF purity, and no contaminating cells were identified. These data support the establishment of quality standards for further Chemistry, Manufacturing, and Controls (CMC) processes.

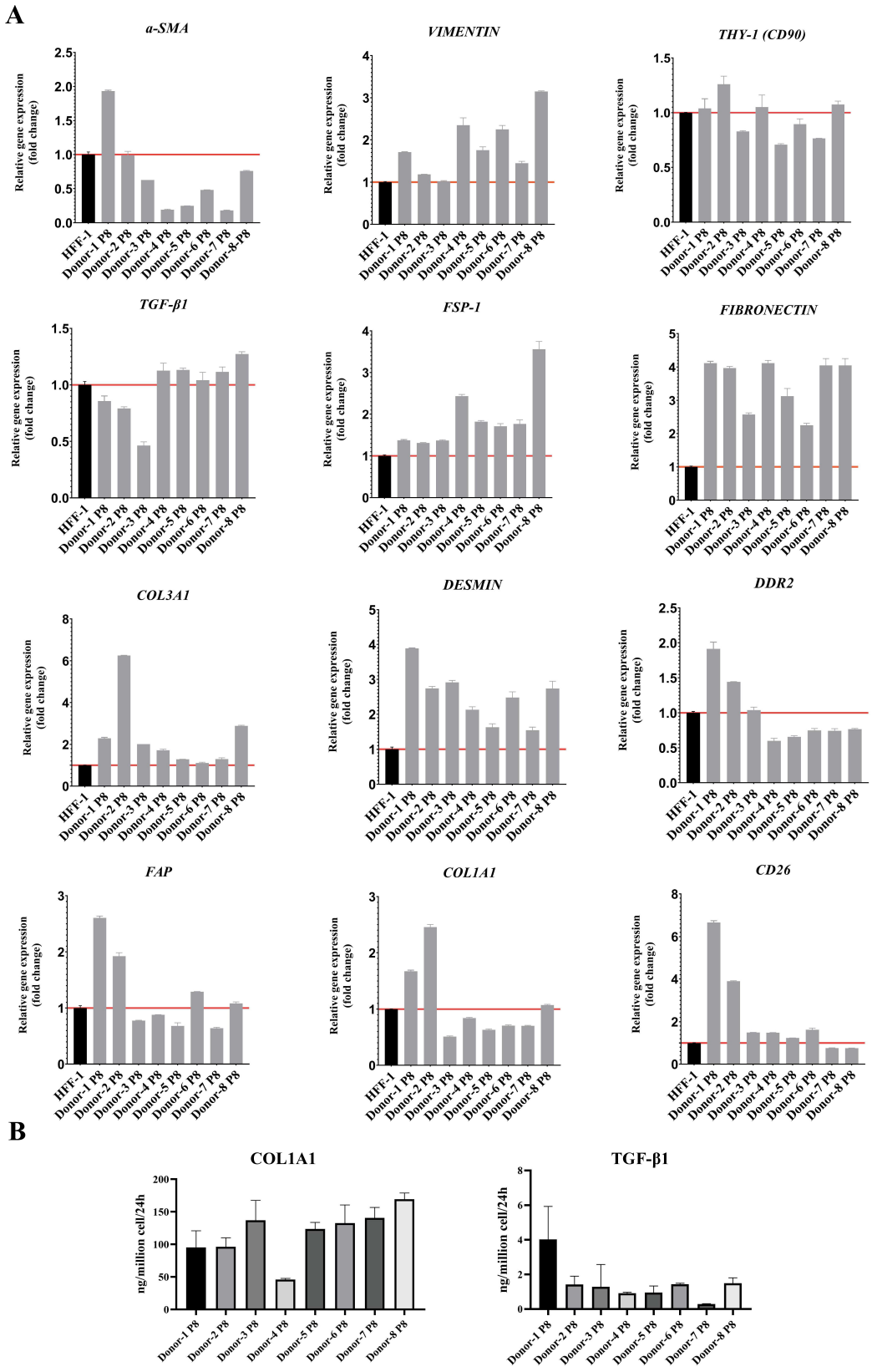

Fig. 4. The gene expression level of human dermal fibroblast. (A) RT-qPCR analysis of α-*SMA*, *VIMENTIN*, *THY-1*, *TGF-*β*1*, *FSP-1*, *FIBRONECTIN*, *COL3A1*, *DESMIN*, *DDR2*, *FAP*, *COL1A1*, and *CD26* gene expression in HDFs isolated from eight donors compared to the HFF-1 cell line. (B) ELISA analysis of TGF-β1 and COL1A1 protein expression in P8 HDFs isolated from eight donors.

Table 1. Protein level expression of 8 batches of HDF production.

Markers	Donor 1	Donor 2	Donor 3	Donor 4	Donor 5	Donor 6	Donor 7	Donor 8
CD105	98.2%	93.81%	93.3%	98.6%	97.3%	97.37%	97.2%	99.1%
CD90	100%	100%	100%	100%	100%	100%	99.9%	100%
CD73	100%	99.91%	100%	99.9%	99.9%	99.95%	100%	100%
FAP	99.4%	94.35%	91.1%	54%	52.3%	97.16%	67.3%	76.6%
Vimentin	100%	99.57%	99.2%	99.9%	98.1%	99.69%	98.7%	99.3%
Fibronectin	100%	99.97%	100%	99.7%	99.9%	99.96%	99.9%	100%
FSP-1	100%	99.01%	99.9%	97.5%	99.7%	99.41%	99.9%	99.9%
α-SMA	100%	99.97%	99.9%	99.7%	99.9%	99.9%	99.9%	100%
Desmin	100%	99.93%	99.9%	99.3%	100%	99.99%	100%	100%
COL1A1	99.8%	99.67%	86.8%	99.9%	92.3%	99.78%	99.4%	96%
CD45	1.19%	0.03%	1.41%	1.62%	1.21%	0.04%	1.44%	1.91%
CD31	2.36%	0.15%	1.56%	1.52%	1.45%	0%	1.41%	1.84%
CD11b	1.28%	0.13%	1.42%	1.89%	0.92%	0.15%	1.44%	1.92%
HLA-DR/DQ/DP	0.94%	0.12%	1.7%	2.35%	1.29%	0.07%	1.33%	1.38%

FAP, fibroblast activation protein; FSP-1, fibroblast specific protein 1; α-SMA, Alpha smooth muscle actin; COL1A1, collagen, type I, alpha 1 chain; HLA-DR/DQ/DP, human leukocyte antigen-DR/DQ/DP.

3.6 Single-Cell Sequencing and Proteomic Analysis of HDF

Single-cell sequencing and proteomic analysis were performed to characterize the phenotype and functions of HDF further. UMAP clustering and subgroup feature analysis indicated that HDF derived from donor 1 and donor 3 exhibited identical subgroup feature distribution and gene expression profiles (Fig. 6A,B), suggesting they belong to the same cell class. The epidermis of the foreskin was removed from the dermal tissue of donor 1, while the whole foreskin tissue was directly digested in donor 3, omitting the epidermis removal process. Through sc-RNAseq, we investigated whether the subtypes of cultured fibroblasts differed after the two kinds of digest process and found that the harvested fibroblasts were identical. Consistent with previous findings (Fig. 3), these data further confirm that the separation of the epidermis does not affect HDF characteristics. The Violin Plot also showed that the gene expression levels of Tgfb1, Col1a1, Col1a2, Col3a1, Thy1 (encoding CD90), *S100A4* (encoding FSP-1), Fn1 (encoding FIBRONECTIN), and Vim (encoding VIMENTIN) were identical in HDFs derived from donor 1 and donor 3. These results align with the flow cytometry analysis and qRT-PCR results (Figs. 4,5,6C).

Post-cultured media was collected and sent for proteomic analysis to identify proteins secreted by cultured cells. Comparing this with the basal medium, we identified 3978 differentially expressed proteins, of which 2439 were significantly up-regulated (Fig. 6D). These significantly differentially expressed proteins were enriched in processes such as peptide biosynthesis, cellular amide metabolism, and macromolecule biosynthesis, highlighting fibroblasts' ability to secrete proteins involved in various biological processes (Fig. 6E). Additionally, a heatmap of fibroblast markers confirmed that foreskin-derived HDF expressed all fibroblast markers (Fig. 6F). Kyoto encyclopedia of genes and genomes (KEGG) pathway analysis revealed that many secreted cytokines were involved in pathways such as basal transcription factors, sphingolipid metabolism, and proteasome function, suggesting HDF's potential for multiple therapeutic functions (Fig. 6G).

3.7 The Xenoplastic Transplantation of HDFs in IVDD Rabbits Mitigates Disc Degeneration

To evaluate the therapeutic effect of HDF on IVDD in rabbits, we adapted the classical needle-puncture-induced IVDD modeling method [27]. Using 20 G needles, we punctured the center of the discs and rotated once. We then injected either solvent alone, or 5×10^5 or 2×10^6 HDFs into the rabbit discs using a micro-syringe. The therapeutic effect of the HDF injection was assessed at 1, 3, and 6 months post-injection.

All animals were anesthetized for MRI and CT imaging, after which the effectiveness of HDFs was evaluated. MRI scan at 1, 3, and 6 months post operation (Post-OP groups) showed a significant decrease in the enhanced signal (gray value) of Intervertebral Discs (IVDs) in the control group (punctured and solvent-injected IVDs), indicating progressive and severe degeneration (Fig. 7A,B). Over time, the signal further decreased, while sham segments showed no obvious IVD degeneration. In contrast, the strengthened signal of the IVDs treated with puncture and HDFs injection showed only a slight decrease within six months. Over time, the rate of degeneration significantly slowed, and the strengthened signal was maintained. This indicates that HDFs injection partly mitigated the degeneration of IVDs (Fig. 7A,B). Moreover, the Disc Height Index (DHI) was maintained in HDF-treated IVDs compared to the control group within six months (Fig. 7C). We previously reported that IVD instability leads to osteophyte for-

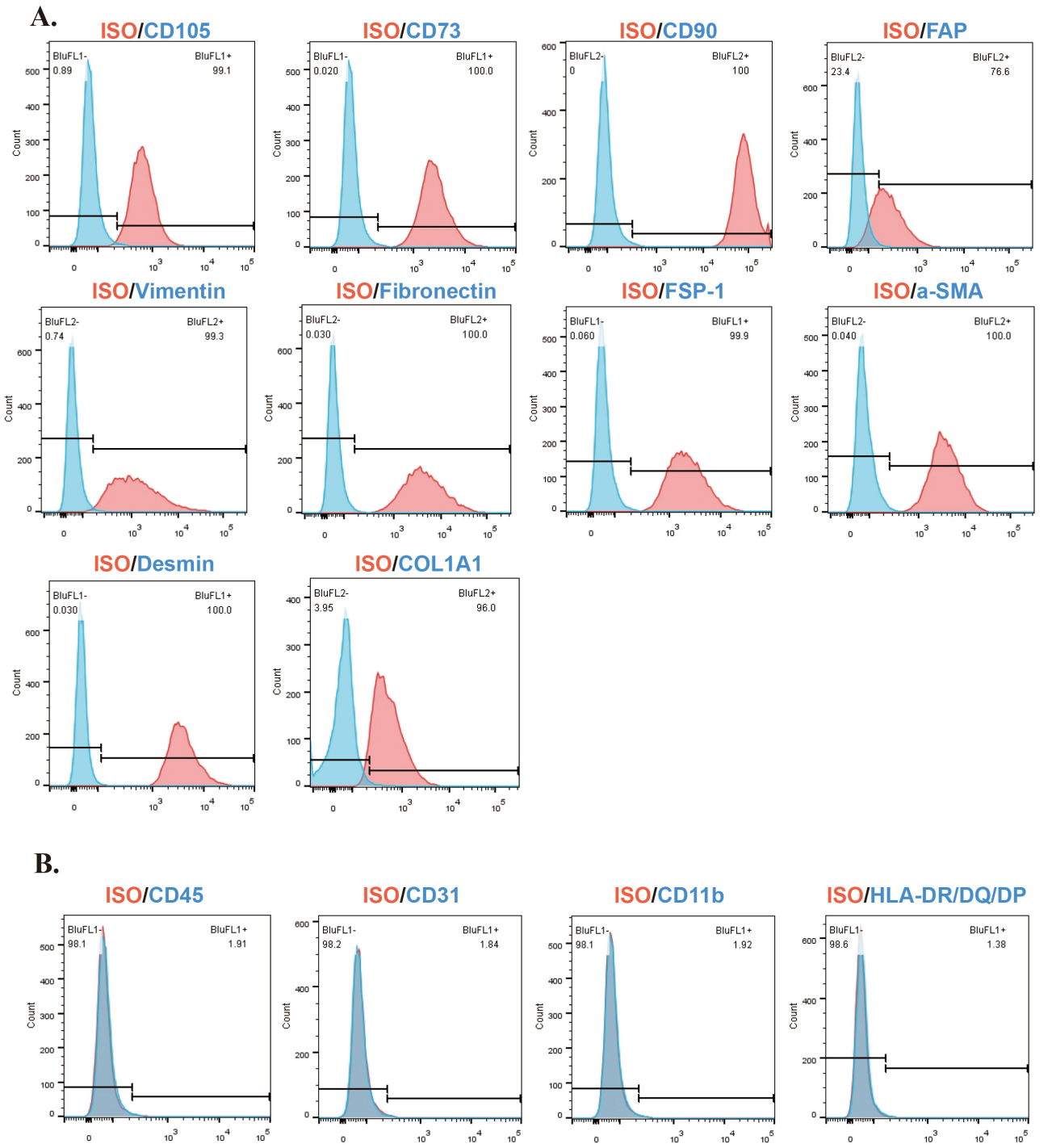

Fig. 5. Positive and negative markers of human dermal fibroblast at P8. (A) Flow cytometry (FCM) analysis of positive markers (CD105, CD73, CD90, vimentin, fibronectin, FSP-1, desmin, and COL1A1) in HDFs at passage 8 (P8). (B) FACS analysis of negative markers (CD45, CD31, CD11b, and HLA-DR/DQ/DP) in HDFs at P8. ISO, isotype.

mation, and allogeneic transplantation of dermal fibroblasts significantly reduced this in rabbits. In this study, CT scans showed that xenoplastic transplantation of HDFs in IVDD rabbits also inhibited osteophyte formation around the intervertebral space, suggesting that HDF treatment helps maintain IVD stability (Fig. 7D,E).

Histological analysis revealed the physiological changes in IVDs. The results of H&E and Safranin O-Fast Green (SOFG) histochemical staining showed that sham IVDs had a well-structured internal nucleus pulposus (NP) and external concentric annulus fibrosus (AF). In contrast, punctured IVDs with solvent showed significant loss of NP tissue and structural collapse. However, IVDs

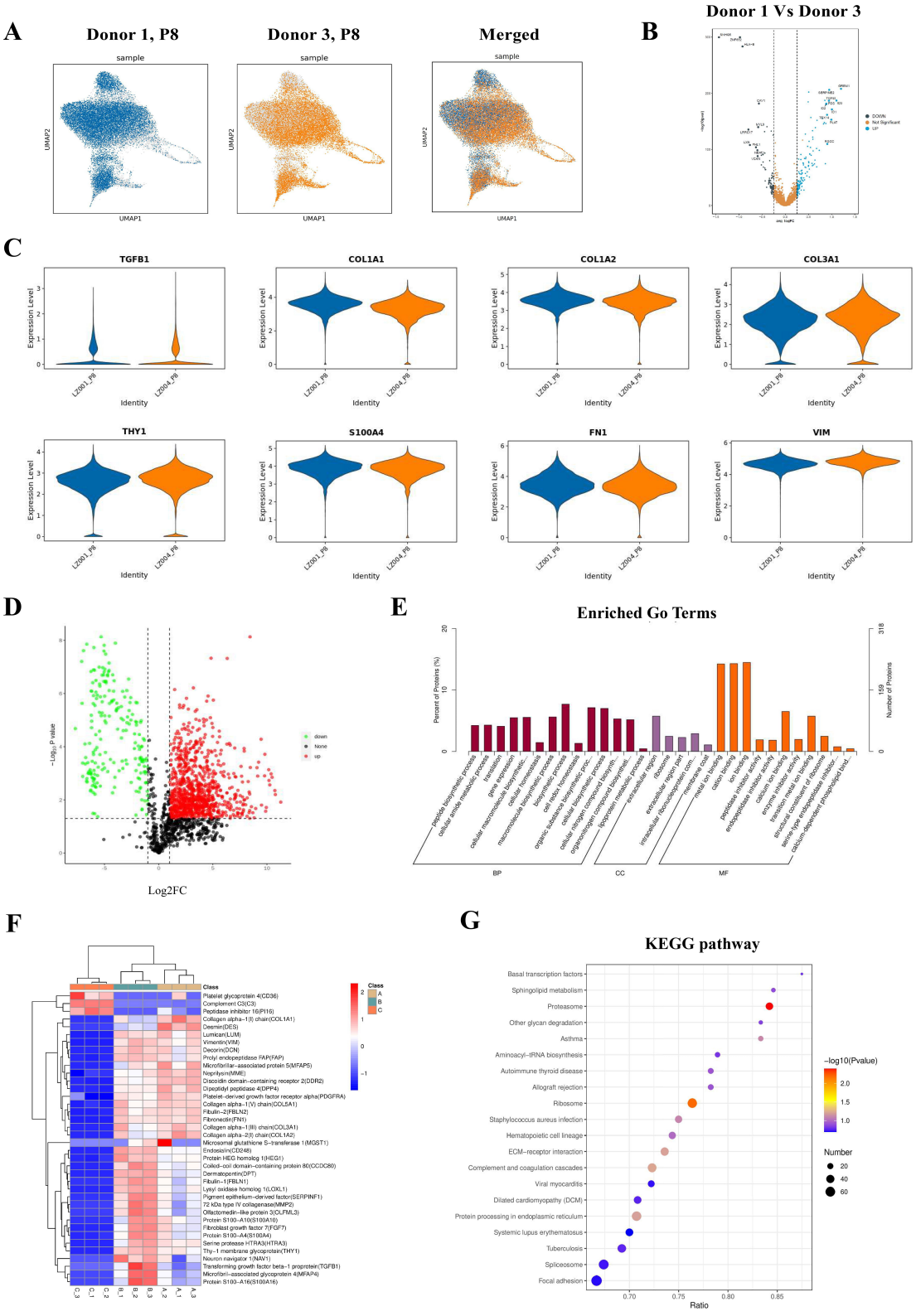

Fig. 6. Single-cell sequencing and proteomic analysis of HDF. (A) UMAP clustering of HDFs isolated from donors 1 and 3. (B) Volcano plot comparing HDFs isolated from donors 1 and 3. (C) Violin plots of single-cell sequencing data showing expression levels of *COL1A1*, *COL1A2*, *COL3A1*, *FIBRONECTIN*, *FSP-1*, *THY-1*, and *VIMENTIN* in HDFs isolated from donors 1 and 3. (D) Volcano plot of proteomic analysis of HDFs. (E) Gene ontology (GO) enrichment analysis from proteomic data of HDFs. (F) Heatmap clustering based on proteomic analysis of HDFs. (G) Kyoto encyclopedia of genes and genomes (KEGG) pathway enrichment analysis from proteomic data of HDFs.

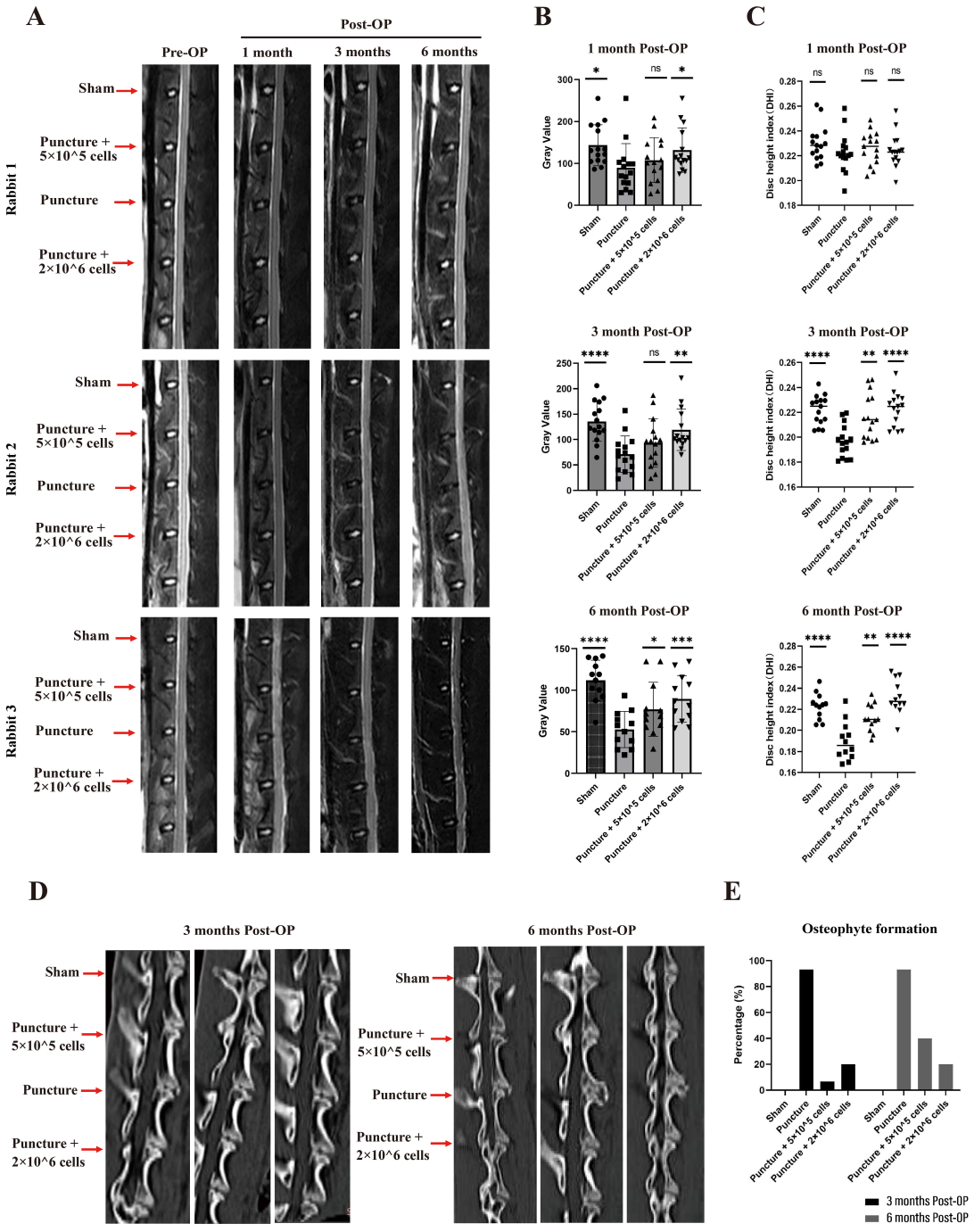

Fig. 7. The therapeutic effect of human dermal fibroblast on treating intervertebral disc degeneration (IVDD) rabbits. (A) Magnetic resonance imaging (MRI) images of rabbit intervertebral discs (IVDs) from the Sham group, Puncture group, and Puncture + Cell Treatment group at 1, 3, and 6 months. (B) Statistical analysis of gray values of rabbit IVDs in the Sham group, Puncture group, and Puncture + Cell Treatment group at 1, 3, and 6 months. The significance is reflected in the comparison between each group and the puncture group (n=15 at 1, 3 months; n=12 at 6 months). (C) Statistical analysis of disc height index (DHI) in rabbit IVDs from the Sham group, Puncture group, and Puncture + Cell Treatment group at 1, 3, and 6 months. The significance is reflected in the comparison between each group and the puncture group (n=15 at 1, 3 months; n=12 at 6 months). (D) Computed tomography (CT) images of osteophyte formation in rabbit IVDs from the Sham group, Puncture group, and Puncture + Cell Treatment group at 3 and 6 months. (E) Statistical analysis of osteophyte formation rates in rabbit IVDs from the Sham group, Puncture group, and Puncture + Cell Treatment group at 3 and 6 months. *ns* > 0.05; *p < 0.05; **p < 0.01; ***p < 0.005; ****p < 0.0001. Post-OP, post operation.

Table 2. Body temperature.

Temperature (°C)	D-1	D1	D3	D5	D8	D15	D22	D29
1M001	38.7	37.3	37.1	37.6	38.5	38.6	37.8	38.2
1F001	38.8	37.1	37.8	38.9	38.7	38.1	38.2	38.9
2M001	39.1	38.4	37.8	38.6	38.4	38.7	38.6	39.1
2F001	38.3	36.0	38.0	36.7	38.2	38.5	37.8	37.4

Table 3. Blood coagulation index.

Blood coagulation index	APTT (s)	APTT (s)	APTT (s)	PT (s)	PT (s)	PT (s)	Fbg C. (g/L)	Fbg C. (g/L)	Fbg C. (g/L)
	D-1	D5	D29	D-1	D5	D29	D-1	D5	D29
1M001	22.80	22.50	23.10	8.10	7.90	8.10	2.23	2.96	2.12
1F001	22.50	22.50	23.50	7.30	7.20	7.30	1.86	2.23	1.69
2M001	26.40	23.50	24.90	8.10	8.10	8.10	1.97	2.29	1.97
2F001	23.80	23.10	24.50	8.00	8.00	8.20	2.66	3.21	3.49

APTT, activated partial thromboplastin time; PT, prothrombin time; Fbg C, fibrinogen C.

treated with HDF maintained a relatively intact structure and did not collapse (Fig. 8A,B). Measuring the height of the IVDs revealed that punctured IVDs with solvent were significantly reduced in height. Meanwhile, the height of HDF-treated IVDs was dose-dependent, corresponding to the amount of HDFs injected (Fig. 8C).

3.8 The Xenoplastic Transplantation of HDFs Increased Disc Fibrosis in Cynomolgus Monkeys

Cynomolgus monkeys (*Macaca fascicularis*) share significant genetic and physiological similarities with humans. To prepare for potential Good Laboratory Practice (GLP) experiments and clinical tests of human dermal fibroblast injection (FibroCell^{TM}), we injected 3×10^6 and 1.2×10^7 cells per IVD in four Cynomolgus monkeys (two low dose and two high dose, Fig. 9). We then monitored their daily status and blood biochemistry for four weeks. No deaths or obvious toxic reactions related to the test substance were observed in any group. Additionally, there were no substantial abnormalities related to the test substance in food intake, hematology, hemagglutination, blood biochemistry, urinalysis, cytokine levels, organ weight and coefficient, general observation, and histopathological examination of the administration site (Tables 2,3,4,5,6,7, BQL in Table 5 indicates below the detection limit).

After four weeks, the animals were euthanized. Anatomical observations revealed no abnormalities related to FibroCell^{TM} injection. One control disc and one HDF-injected disc were removed from each monkey, and the nucleus pulposus (NP) and annulus fibrosus (AF) were separated for RNA sequencing. Comparison of RNA sequencing data from injected and non-injected IVDs showed no significant change in fibrotic gene expression in the injected and non-injected AF tissues, indicating that FibroCell^{TM} injection mainly affects NPs. Most fibrosis genes in NP tissues at the injection site were significantly up-regulated compared to the non-injection site. This indicates that HDF injections induce fibrosis in NP tissues, potentially providing structural support (Fig. 9). These findings offer strong evidence for studying the mechanism and safety of HDF injection in treating IVDD.

Table 4. Electrocardiogram data.

Day	Animal ID	PR	QRS	QT	RR	HR
D-1	2M001	0.08	0.04	0.17	0.26	230
D-1	2F001	0.06	0.04	0.18	0.24	250
D-1	1M001	0.07	0.04	0.15	0.24	250
D-1	1F001	0.08	0.04	0.20	0.28	218
D1	1M001	0.07	0.04	0.19	0.27	232
D1	1F001	0.07	0.04	0.20	0.26	234
D1	2M001	0.08	0.04	0.17	0.25	237
D1	2F001	0.08	0.04	0.21	0.28	216
D28	1M001	0.08	0.04	0.16	0.24	245
D28	1F001	0.08	0.04	0.20	0.24	227
D28	2M001	0.08	0.04	0.16	0.24	239
D28	2F001	0.08	0.04	0.16	0.24	227

ID, identity document; PR, P-R interval; QRS, QRS wave complex; QT, Q-T interval; RR, Respiratory Rate; HR, heart rate.

4. Discussions

Currently, the primary treatment for degenerative disc disease involves conservative methods, often supplemented by surgical interventions. Conservative treatment primarily encompasses drug therapy (primarily for pain relief), lumbar fixation, physical therapies such as traction massage, and "closed" treatment. Surgical treatment is necessary when conservative methods are ineffective, if there is neurological deterioration (such as muscle strength decline, atrophy, etc.), or even cauda equina syndrome (perineal numbness, urination, and defecation disorders). Surgical interventions are typically designed to maintain the stability of the intervertebral space and alleviate severe neurological symptoms. This often includes discectomy and interbody fusion. However, nucleus pulposus removal may pose the

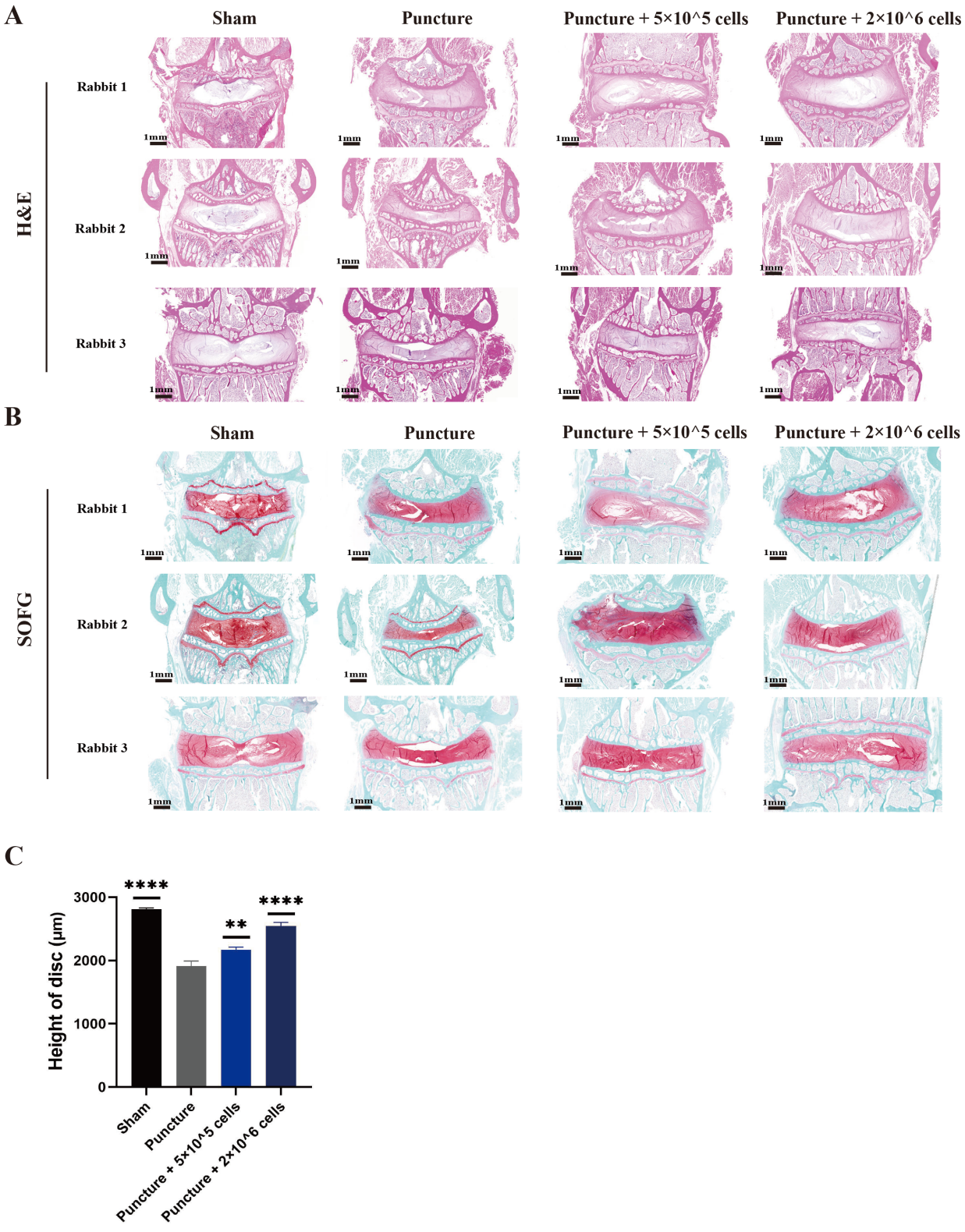

Fig. 8. The histological analysis of intervertebral discs after treatment. (A) Hematoxylin and eosin (H&E) staining of rabbit IVDs from the Sham group, Puncture group, and Puncture + Cell Treatment group at 3 months. Scale bars, 1 mm. (B) Safranin O and fast green (SOFG) staining of rabbit IVDs from the Sham group, Puncture group, and Puncture + Cell Treatment group at 3 months. Scale bars, 1 mm. (C) Measurement and statistical analysis of IVD heights in rabbits from the Sham group, Puncture group, and Puncture + Cell Treatment group at 3 months. $^{**}p < 0.01$; $^{****}p < 0.0001$.

Table 5. Inflammatory cytokine level.

		IFN-γ	IL-2	IL-6	TNF-α			IFN-γ	IL-2	IL-6	TNF-α
Pre-injection	1F001	BQL	BQL	BQL	BQL	4 h	1F001	BQL	BQL	BQL	BQL
	1M001	BQL	BQL	3.31	BQL		1M001	BQL	BQL	3.58	BQL
	2F001	BQL	BQL	5.60	BQL		2F001	BQL	BQL	2.93	BQL
	2M001	BQL	BQL	1.53	BQL		2M001	BQL	BQL	1.12	BQL
		IFN-γ	IL-2	IL-6	TNF-α			IFN-γ	IL-2	IL-6	TNF-α
24 h	1F001	BQL	BQL	BQL	BQL	D29	1F001	BQL	BQL	BQL	BQL
	1M001	BQL	BQL	BQL	BQL		1M001	BQL	BQL	BQL	BQL
	2F001	BQL	BQL	BQL	BQL		2F001	BQL	BQL	BQL	BQL
	2M001	BQL	BQL	BQL	BQL		2M001	BQL	BQL	BQL	BQL

IFN-γ, interferon-γ; BQL, below the quantization limit; TNF-α, tumour necrosis factor-alpha.

Table 6. Organ coefficient.

	Heart/brain (%)	Liver (with gallbladder)/ brain (%)	Spleen/ brain (%)	Kidney/ brain (%)	Thymus/ brain (%)	Renicapsule/ brain (%)	Thyroid & parathyroid bodies/brain (%)
1M001	16.2158	70.3583	4.4470	16.6549	6.5855	0.8214	0.6231
1F001	23.9379	109.3849	3.9949	25.3171	1.9023	0.8402	0.6975
2M001	25.1690	99.7695	4.7173	22.2803	2.1973	1.0910	0.4610
2F001	18.4814	87.7587	3.9637	19.2455	2.8972	0.9710	0.3025

Table 7. Blood biochemical index.

Blood biochemical index	AST (U/L)	AST (U/L)	CK (U/L)	CK (U/L)	ALP (U/L)	ALP (U/L)	UREA (mM)	UREA (mM)	LDH (U/L)	LDH (U/L)	CRP (mg/L)	CRP (mg/L)
	D-1	D29	D-1	D29	D-1	D29	D-1	D29	D-1	D29	D-1	D29
1M001	56.2	57.4	286	312	469.8	376.5	7.62	6.10	763	756	3.0	2.2
1F001	64.6	34.8	405	120	127.4	85.6	5.97	3.68	945	543	5.5	1.5
2M001	55.1	55.2	159	153	399.3	318.6	7.16	5.93	682	615	2.6	2.3
2F001	60.7	54.8	287	245	188.3	202.4	6.24	5.44	732	558	1.1	1.3

AST, aspartate aminotransferase; CK, creatine kinase; ALP, alkaline phosphatase; LDH, lactate dehydrogenase; CRP, c-reactive protein.

risk of recurrent disc herniation and could potentially lead to a loss of intervertebral space height over time. Intervertebral disc fusion necessitates the sacrifice of the patient's lumbar spine activity and may accelerate the degeneration of adjacent intervertebral discs due to the increased biomechanical load.

Although current treatment methods can alleviate pain, they are unable to supplement the extracellular matrix of the intervertebral disc, repair damaged AF and NP tissue, restore the height of the intervertebral disc, or inhibit inflammation within the intervertebral disc. Consequently, these methods cannot cure disc degeneration. The complications and disadvantages are evident, and there are few alternative treatments for patients who have failed conservative treatment for degenerative disc disease. Given the unmet clinical application needs and market gaps, fibroblast therapy emerges as a promising approach to manage disc degeneration and effectively address the mid-stage of disc degenerative diseases.

Our team specializes in non-surgical treatments for IVDD. Through extensive clinical cases and histological examinations, we found that elevated pro-fibrotic markers in IVDD patients' tissues and the long-term prognosis of PELD are linked to the disc fibrosis level. At a cell-biological level, nucleus pulposus cells are induced to adopt a pro-fibrotic phenotype, increasing the expression of fibrotic markers such as COL1a1, COL3a1, VIMENTIN, FSP1, among others. Chemicals like bleomycin and pre-fibrotic cell types, such as fibroblasts [20], intensify the fibrosis phenotype in degenerative discs, thereby maintaining the stability of degenerative intervertebral discs and reducing osteophytes in the long term [21]. Fibroblast injection offers a promising direction for treating intervertebral space-derived lumbar degenerative diseases.

In this study, we undertook a QbD project to develop a human dermal skin-derived allogeneic fibroblast injection called FibroCell^{TM}. To achieve this, we initially examined the isolation method of human dermal fibroblasts. We then tested several animal-component-free serums as alternatives to FBS and selected seven basal media to determine the most suitable cultural media for human foreskin-derived fibroblasts (Figs. 1,2). We found that hPL is the op-

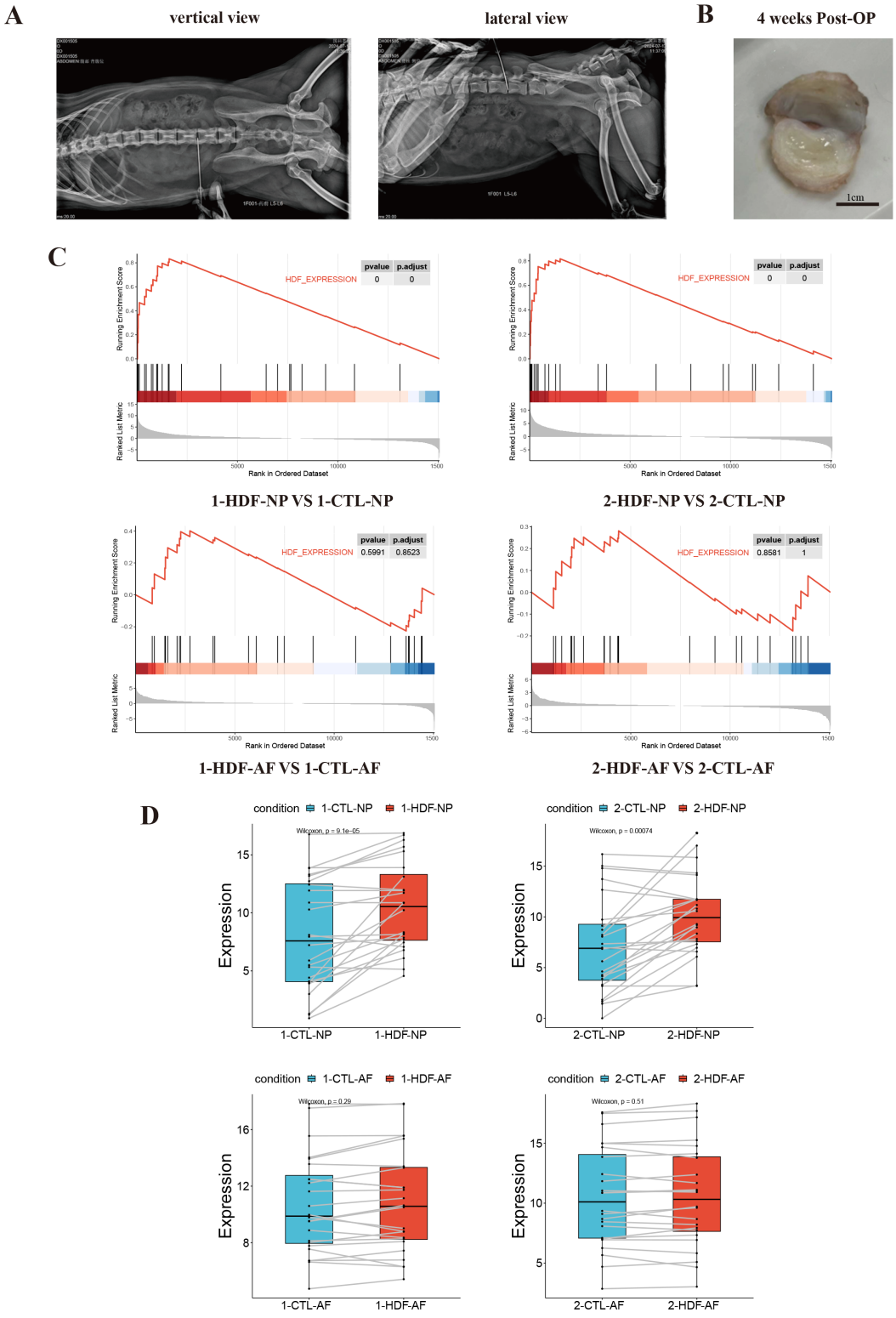

Fig. 9. HDF injection increased disc fibrosis in cynomolgus monkeys. (A) Vertical and lateral views of HDF injection in cynomolgus monkeys. (B) Illustration of the intervertebral disc (IVD) incision at the injection site in cynomolgus monkeys. Scale bars, 1 cm. (C) Gene Set Enrichment Analysis (GSEA) of the nucleus pulposus (NP) and annulus fibrosus (AF) in the injected and healthy regions of IVDs. (D) Differential gene expression analysis in the nucleus pulposus (NP) and annulus fibrosus (AF) between injected and healthy regions of IVDs.

timal FBS substitute for HDF, and DMEM with high glucose was confirmed as the best basal medium. The supplement concentration was adjusted, with HDF cultured in DMEM with 7.5% hPL yielding the highest cell count with the shortest doubling time (Fig. 2E,F). The seeding cell numbers ranged between 14,000/cm^2 and 18,000/cm^2 (Fig. 2G–I). Additionally, 75% CS-10 + 10% HSA + 15% NaCl (v/v) was identified as the best freezing solution for HDF (Fig. 2J,K). Furthermore, the proliferation rate, gene expression levels, and protein markers of all 8 donors of HDF were consistent (Figs. 3,4,5), regardless of whether the epidermis was removed or not, indicating that our production methods are reliable. Single-cell sequencing and proteomic analysis have confirmed the purity of HDF. Additionally, these analyses have identified the involvement of numerous cytokines in the treatment of various diseases (Fig. 6).

Therefore, we developed a GMP-compliant procedure to produce clinical-scale human dermal-skin-derived fibroblast and validated the process stability through eight small-scale batches. The cell characteristics and quality control were assessed using qRT-PCR, FACS analysis, and single-cell sequencing. The therapeutic effects of FibroCell^{TM} were demonstrated using a stress-induced IVDD model in New Zealand rabbits (Oryctolagus cuniculus) (Figs. 7,8). Safety tests were conducted in Cynomolgus monkeys (*Macaca fascicularis*) (Fig. 9). Results showed that, six months post-injection, HDF restored IVD signal, maintained DHI, and reduced osteophyte formation. The primary mechanism involves secreting extracellular matrix (ECM) and inhibiting degeneration-induced inflammation and neuron formation (data not shown). Further experiments, such GLP experiments, should be conducted using larger animal models to further evaluate the safety and therapeutic effects of HDF injection. This will provide a stronger foundation for advancing these cells to clinical trials.

Cell therapy for IVDD mainly includes fibroblasts and mesenchymal stem cells (MCSs). Although MSCs are widely used and many positive studies are showing that they are promising in the treatment of IVDD [28–30], the short duration of MSCs and the lack of long-lasting efficacy of MSCs are the main challenges in the hypoxic and inflammatory environment. In addition, MSCs only exert a medicinal effect by inhibiting intervertebral disc inflammation, while fibroblasts can not only inhibit inflammation (data not shown), but also restore intervertebral disc height and stability through fibrosis repair, and play a role in structural support.

Our team previously reported that the expression of fibrosis genes in the nucleus pulposus tissue of patients undergoing nucleus pulposus extraction surgery (PELD) increased and that the prognosis of PELD patients was directly related to the degree of intervertebral disc fibrosis [31]. That clinical phenomenon suggests that the long-term prognosis of patients undergoing nucleus pulposus extraction surgery may be related to the degree of intervertebral disc fibrosis, and the concept of fibroblast-induced degenerative disc fibrosis to maintain the height and stability of the intervertebral disc was proposed [20,21]. Our project translates this research into the development of FibroCell products based on the QbD concept for the treatment of degenerative disc diseases. Our team has initiated an investigator-initiated trial in Shanghai, China, and the majority of the twelve volunteers reported relief of low back pain, which might be related to the enhanced fibrosis and structural support of degenerative discs. These clinical data will be reported after follow-up.

5. Conclusions

In this research, we launched a quality-by-design (QbD) project focusing on human dermal fibroblasts to develop a novel human allogenic fibroblast injection. We then explored its therapeutic effects on treating IVDD in rabbits. Signal pathway analysis in cynomolgus monkeys suggested that the primary mechanism involves promoting disc fibrosis. Therefore, this study demonstrated the feasibility and cost-effectiveness of manufacturing FibroCell^{TM}, a foreskin-derived human dermal fibroblast injection. FibroCell^{TM} shows promise as a cell-based therapy for IVDD treatment.

Availability of Data and Materials

The datasets used and/or analyzed during the current study are available from the corresponding author upon reasonable request.

Author Contributions

Conceptualization: SAZ, JZ, and AQ; data acquisition: LZ, HSL, CC, HY, GCZ, QZ, MNW, LS, and TX; data analysis: MF, SAZ, LZ, and JZ; original draft preparation: LZ and HSL; review and editing: SAZ, JZ, AQ, MF, and LZ; all authors revised and agreed on the final version of the manuscript. All authors have participated sufficiently in the work and agreed to be accountable for all aspects of the work. All authors contributed to editorial changes in the manuscript.

Ethics Approval and Consent to Participate

The study design and volunteer recruitment were approved by the Ethics Committee of the Shanghai Ninth People's Hospital, Shanghai Jiao Tong University School of Medicine (approval number: SH9H-2021-T94-2 and SH9H-2023-T186-3 for the collection of foreskins). The study was carried out in accordance with the guidelines of the Declaration of Helsinki. A written consent was signed by the patients or their families/legal guardians. The animal experiments were approved by the Jiagan Biotechnology Corporation Animal Committee approval number JGLL-

20220601 for rabbits and were approved by the SAFE Medical Technology Co., Ltd. Animal Committee approval number IACUC-2024-538 for cynomolgus monkeys. All experiments adhered to relevant guidelines and regulations.

Acknowledgment

The authors would like to express their gratitude to EditSprings (https://www.editsprings.cn) for the expert linguistic services provided and to all the peer reviewers for their opinions and suggestions.

Funding

The work was supported by FibroX Therapeutics (Shanghai) Inc.

Conflict of Interest

Li Zhou, Hao Yang, Guicheng Zhang, Qin Zhang, Mengnan Wen, Ming Fan, Shen'ao Zhou are all affiliated with FibroX Therapeutics (Shanghai) Inc. All authors declare no conflicts of interest. Despite they received sponsorship from FibroX Therapeutics (Shanghai) Inc, the judgments in data interpretation and writing were not influenced by this relationship.

Supplementary Material

Supplementary material associated with this article can be found, in the online version, at https://doi.org/10.31083/FBL28062.

References

[1] Hill PG. Low back pain. The New England Journal of Medicine. 2001; 344: 1644; author reply 1644–1645.

[2] Ravindra VM, Senglaub SS, Rattani A, Dewan MC, Härtl R, Bisson E, *et al*. Degenerative Lumbar Spine Disease: Estimating Global Incidence and Worldwide Volume. Global Spine Journal. 2018; 8: 784–794. https://doi.org/10.1177/2192568218770769.

[3] Singla AK, Stojanovic M, Barna S. Persistent low back pain. The New England Journal of Medicine. 2005; 353: 956–956–7; author reply 956–957. https://doi.org/10.1056/NEJMc051504.

[4] Maher C, Underwood M, Buchbinder R. Non-specific low back pain. Lancet (London, England). 2017; 389: 736–747. https://doi.org/10.1016/S0140-6736(16)30970-9.

[5] Choi YS. Pathophysiology of degenerative disc disease. Asian Spine Journal. 2009; 3: 39–44. https://doi.org/10.4184/asj.2009.3.1.39.

[6] Urban JPG, Roberts S. Degeneration of the intervertebral disc. Arthritis Research & Therapy. 2003; 5: 120–130. https://doi.org/10.1186/ar629.

[7] Wilkens P, Scheel IB, Grundnes O, Hellum C, Storheim K. Effect of glucosamine on pain-related disability in patients with chronic low back pain and degenerative lumbar osteoarthritis: a randomized controlled trial. JAMA. 2010; 304: 45–52. https://doi.org/10.1001/jama.2010.893.

[8] Sun Y, Zhao YB, Pan SF, Zhou FF, Chen ZQ, Liu ZJ. Comparison of adjacent segment degeneration five years after single level cervical fusion and cervical arthroplasty: a retrospective controlled study. Chinese Medical Journal. 2012; 125: 3939–3941.

[9] Sztrolovics R, Alini M, Roughley PJ, Mort JS. Aggrecan degradation in human intervertebral disc and articular cartilage. The Biochemical Journal. 1997; 326 (Pt 1): 235–241. https://doi.org/10.1042/bj3260235.

[10] Donohue PJ, Jahnke MR, Blaha JD, Caterson B. Characterization of link protein(s) from human intervertebral-disc tissues. The Biochemical Journal. 1988; 251: 739–747. https://doi.org/10.1042/bj2510739.

[11] Gomes RN, Manuel F, Nascimento DS. The bright side of fibroblasts: molecular signature and regenerative cues in major organs. NPJ Regenerative Medicine. 2021; 6: 43. https://doi.org/10.1038/s41536-021-00153-z.

[12] Plikus MV, Wang X, Sinha S, Forte E, Thompson SM, Herzog EL, *et al*. Fibroblasts: Origins, definitions, and functions in health and disease. Cell. 2021; 184: 3852–3872. https://doi.org/10.1016/j.cell.2021.06.024.

[13] Seki S, Iwasaki M, Makino H, Yahara Y, Miyazaki Y, Kamei K, *et al*. Direct Reprogramming and Induction of Human Dermal Fibroblasts to Differentiate into iPS-Derived Nucleus Pulposus-like Cells in 3D Culture. International Journal of Molecular Sciences. 2022; 23: 4059. https://doi.org/10.3390/ijms23074059.

[14] Sheyn D, Ben-David S, Tawackoli W, Zhou Z, Salehi K, Bez M, *et al*. Human iPSCs can be differentiated into notochordal cells that reduce intervertebral disc degeneration in a porcine model. Theranostics. 2019; 9: 7506–7524. https://doi.org/10.7150/thno.34898.

[15] Qian H, He L, Ye Z, Wei Z, Ao J. Decellularized matrix for repairing intervertebral disc degeneration: Fabrication methods, applications and animal models. Materials Today Bio. 2023; 18: 100523. https://doi.org/10.1016/j.mtbio.2022.100523.

[16] Specchia N, Pagnotta A, Toesca A, Greco F. Cytokines and growth factors in the protruded intervertebral disc of the lumbar spine. European Spine Journal: Official Publication of the European Spine Society, the European Spinal Deformity Society, and the European Section of the Cervical Spine Research Society. 2002; 11: 145–151. https://doi.org/10.1007/s00586-001-0361-y.

[17] Xu X, Zheng L, Yuan Q, Zhen G, Crane JL, Zhou X, *et al*. Transforming growth factor-β in stem cells and tissue homeostasis. Bone Research. 2018; 6: 2. https://doi.org/10.1038/s41413-017-0005-4.

[18] Chee A, Shi P, Cha T, Kao TH, Yang SH, Zhu J, *et al*. Cell Therapy with Human Dermal Fibroblasts Enhances Intervertebral Disk Repair and Decreases Inflammation in the Rabbit Model. Global Spine Journal. 2016; 6: 771–779. https://doi.org/10.1055/s-0036-1582391.

[19] Shi P, Chee A, Liu W, Chou PH, Zhu J, An HS. Therapeutic effects of cell therapy with neonatal human dermal fibroblasts and rabbit dermal fibroblasts on disc degeneration and inflammation. The Spine Journal: Official Journal of the North American Spine Society. 2019; 19: 171–181. https://doi.org/10.1016/j.spinee.2018.08.005.

[20] Chen C, Zhou T, Sun X, Han C, Zhang K, Zhao C, *et al*. Autologous fibroblasts induce fibrosis of the nucleus pulposus to maintain the stability of degenerative intervertebral discs. Bone Research. 2020; 8: 7. https://doi.org/10.1038/s41413-019-0082-7.

[21] Chen C, Huang Y, Shi L, Zhou L, Zhou S, Wan H, *et al*. Allogeneic fibroblasts ameliorate intervertebral disc degeneration by reducing osteophytes in rabbits. Frontiers in Medicine. 2024; 11: 1488727. https://doi.org/10.3389/fmed.2024.1488727.

[22] Williams R, Thornton MJ. Isolation of Different Dermal Fibroblast Populations from the Skin and the Hair Follicle. Methods in Molecular Biology (Clifton, N.J.). 2020; 2154: 13–22. https://doi.org/10.1007/978-1-0716-0648-3_2.

[23] Pakshir P, Alizadehgiashi M, Wong B, Coelho NM, Chen X, Gong Z, *et al*. Dynamic fibroblast contractions attract remote macrophages in fibrillar collagen matrix. Na-

ture Communications. 2019; 10: 1850. https://doi.org/10.1038/s41467-019-09709-6.

[24] Khalid S, Ekram S, Salim A, Chaudhry GR, Khan I. Transcription regulators differentiate mesenchymal stem cells into chondroprogenitors, and their *in vivo* implantation regenerated the intervertebral disc degeneration. World Journal of Stem Cells. 2022; 14: 163–182. https://doi.org/10.4252/wjsc.v14.i2.163.

[25] Kahounová Z, Kurfürstová D, Bouchal J, Kharaishvili G, Navrátil J, Remšík J, *et al*. The fibroblast surface markers FAP, anti-fibroblast, and FSP are expressed by cells of epithelial origin and may be altered during epithelial-to-mesenchymal transition. Cytometry. Part a: the Journal of the International Society for Analytical Cytology. 2018; 93: 941–951. https://doi.org/10.1002/cyto.a.23101.

[26] Amit M, Margulets V, Segev H, Shariki K, Laevsky I, Coleman R, *et al*. Human feeder layers for human embryonic stem cells. Biology of Reproduction. 2003; 68: 2150–2156. https://doi.org/10.1095/biolreprod.102.012583.

[27] Han B, Zhu K, Li FC, Xiao YX, Feng J, Shi ZL, *et al*. A simple disc degeneration model induced by percutaneous needle puncture in the rat tail. Spine. 2008; 33: 1925–1934. https://doi.org/10.1097/BRS.0b013e31817c64a9.

[28] Bates D, Vivian D, Freitag J, Wickham J, Mitchell B, Verrills P, Young JF. Low-dose mesenchymal stem cell therapy for discogenic pain: safety and efficacy results from a 1-year feasibility study. Future Science OA. 2022; 8: FSO794.

[29] Henry N, Clouet J, Le Bideau J, Le Visage C, Guicheux J. Innovative strategies for intervertebral disc regenerative medicine: From cell therapies to multiscale delivery systems. Biotechnology Advances. 2018; 36: 281–294. https://doi.org/10.1016/j.biotechadv.2017.11.009.

[30] Hunt CL, Shen S, Nassr A, van Wijnen AJ, Larson AN, Eldrige JS, *et al*. Current understanding of safety and efficacy of stem cell therapy for discogenic pain—A systematic review of human studies. Techniques in Regional Anesthesia and Pain Management. 2015; 19: 32–37.

[31] Yang X, Chen Z, Chen C, Han C, Zhou Y, Li X, *et al*. Bleomycin induces fibrotic transformation of bone marrow stromal cells to treat height loss of intervertebral disc through the TGFβR1/Smad2/3 pathway. Stem Cell Research & Therapy. 2021; 12: 34. https://doi.org/10.1186/s13287-020-02093-9.